SIMULATION OF EXTREME EVENTS OF OBLIQUE WAVE INTERACTION WITH POROUS BREAKWATER STRUCTURES

Bjarne Jensen[1], Erik Damgaard Christensen[2], Niels Gjøl Jacobsen[3]

This paper introduces a numerical approach for the analysis of extreme events of wave interaction with coastal and marine structures. The method is exemplified by investigating oblique wave interactions with a rubble mound breakwater structure. The use of numerical models for analysis of wave-structure interaction is seen more often. For many applications a two-dimensional approximation is valid, however, for investigating complex structural details or e.g. oblique wave interaction with coastal structures, a three-dimensional simulation is required. One challenge for a practical use of three-dimensional simulations is the computational cost. For extreme event analysis it is necessary to determine the characteristics of the extreme events which will occur during an irregular sea state of a given duration. Therefore the complete irregular sea state must be simulated. A three-dimensional simulation of a full irregular sea state with duration of e.g. 3 hours will be a large computational burden. The present work proposes a methodology where the analysis is performed in two steps. 1) A two-dimensional simulation of a full 3 hour irregular sea state is performed including the breakwater structure. The extreme events are observed in terms of loads on the super-structure. 2) The extreme events are reproduced in a three-dimensional model as oblique waves by short realizations. The method was validated by comparing the surface elevation and sea-wall forces from a full irregular sea state to the short reproduction sequences. Good agreement was found for both surface elevation and horizontal sea-wall forces. The short reproduction of extreme events was applied in a three-dimensional setup for investigating the effect of oblique waves. For an incident wave angle of 30° a reduction of the peak impact load of 25 – 50 % was found for the tested extreme events.

Keywords: Wave-structure interaction; Extreme events; Rubble mound breakwaters; Porous media; Navier-stokes equations; OpenFoam

INTRODUCTION

In the field of coastal engineering the use of computational fluid dynamics (CFD) has gained more popularity in the recent years. The possibility to include the effect of porous media such as rubble mound breakwaters and the description of free surface water waves have enhanced the applicability of CFD within coastal engineering. The extension of the numerical models to handle porous media was presented in van Gent (1995) where the effect of the porous media was included in the Navier-Stokes equations based on a resistance term. This method has been developed in e.g. Liu et al. (1999) and Hsu (2002). Recent examples of the development and application of this type of porosity models are del Jesus et al. (2012), Lara et al. (2012a) and Higuera et al. (2014a). In Jensen et al. (2014) the detailed derivation of the porous media equations was presented together with the most recent version of the equations implemented in the open source CFD library OpenFoam®. Together with the wave generation capabilities presented in Jacobsen et al. (2012) the OpenFoam model has contributed to the availability of open source CFD for coastal engineering topics. Examples of the use of OpenFoam for considering both flow in connection with breakwaters, modelling of scour around structures, and cross-shore morphodynamics were recently seen in for example Lara et al. (2012b), Matsumoto et al. (2012), Stahlmann and Schlurmann (2012), Jacobsen and Fredsøe (2014), and Higuera et al. (2014b).

For three-dimensional prototype applications one of the limiting factors is the computational time. In the case where irregular sea states are being considered it may be impossible seen from a practical engineering perspective to conduct a detailed CFD analysis. For fatigue analyses the entire irregular time series must be included in the simulations, however, for extreme events and ultimate-limit-state (ULS) analysis only a few very short events are of interest. For these cases the methodology presented in this paper may contribute to enhancing the efficiency of the CFD analysis for practical applications. The method combines a two-dimensional screening model including the entire irregular sea state and a three-dimensional model where only the extreme event of interest is reproduced. The key point in that respect is the ability of the model to simulate the extreme event as a very short sequence of the irregular time series.

The focus of the work presented in this paper was to validate the method for reproducing extreme events from irregular time series. The short reproductions of extreme events were applied for investigating the effect of oblique waves on the forces on a breakwater sea-wall. Previously a numerical investigation of the effect of oblique waves on a vertical impermeable breakwater was presented in Lara et al. (2012b)

[1]Department of Mechanical Engineering, Technical University of Denmark, bjaje@mek.dtu.dk
[2]Department of Mechanical Engineering, Technical University of Denmark, edch@mek.dtu.dk
[3]Coastal Structures and Waves, Deltares, The Netherlands, niels.jacobsen@deltares.nl

however this included regular waves. The effect of extreme events due to the interaction of the irregular waves was not investigated. In Higuera et al. (2014b) a short sequence of an irregular sea state was also applied to investigate oblique wave-interaction with a vertical breakwater however, the applicability of the method and the accuracy of the reproduction in short sequences was not addressed.

The remainder of this paper is organised as follows. First, the numerical model is described including the extension of the model to handle porous media for representing the breakwater structure. Following this, a short note is given on the statistical crest height distribution of the irregular sea state in the model compared to empirical distributions. The two-dimensional screening is conducted in the following section where the rubble mound breakwater is exposed to the entire three hour irregular sea state. The forces on the sea-wall is computed throughout the simulation and from this a number of impact events are chosen to be investigated for oblique wave interactions. The next section performs a validation of the method of reproducing the extreme impact event as a short sequence where the irregular sea state is started with a phase offset. Finally, the same reproduction in short sequences are performed in a three-dimensional model where the waves are generated as oblique waves relative to the breakwater. Conclusions are given in the last section.

NUMERICAL MODEL

The model was based on the Navier-Stokes equations, that were transformed to the Volume Averaged Navier-Stokes equations for including the effect of the porosity. The numerical method was based on a finite volume discretisation on a collocated grid arrangement. The present paper used a version of the Navier-Stokes equations where the eddy viscosity was not taken into account; for a formulation of turbulence closures in porous media, the reader is referred to the literature, e.g. Antohe and Laget (1997) and Nakayama and Kuwahara (1999).

The starting point was the general form of the incompressible Navier-Stokes equations formulated with the continuity equation:

$$\frac{\partial u_i}{\partial x_i} = 0 \tag{1}$$

and the momentum equation:

$$\frac{\partial \rho u_i}{\partial t} + \frac{\partial \rho u_i u_j}{\partial x_j} = -\frac{\partial p}{\partial x_i} - g_j x_j \frac{\partial \rho}{\partial x_i} + \frac{\partial}{\partial x_j}\mu\left(\frac{\partial u_i}{\partial x_j} + \frac{\partial u_j}{\partial x_i}\right) \tag{2}$$

where ρ is the density of the fluid, u_i is the Cartesian velocity vector $u_i = (u, v, w)$, p is the excess pressure, g_j is the j^{th} component of the gravitational vector, μ is the dynamical viscosity, t is the time, and x_i are the Cartesian coordinates.

If Eq. (1) and (2) are to be solved in the porous media, knowledge is required about the geometry of the pores forming the porous media. Furthermore, a very finely resolved computational mesh would be required in order to capture this geometry, which in most cases is not feasible. To overcome this problem the Navier-Stokes equations were averaged over a volume that was assumed to be larger than the length scale of the pores constituting the porous media. A detailed description of the derivation of the volume averaged equations for porous media is presented in Jensen et al. (2014). In the following the final form of the continuity and momentum equations for porous media flow are presented.

The volume averaged continuity equation was given as:

$$\frac{\partial \langle \overline{u}_i \rangle}{\partial x_i} = 0 \tag{3}$$

where $\langle \overline{u}_i \rangle$ is the volume averaged ensemble averaged velocity over the total control volume including the solids of the porous media. The volume averaged momentum equation was formulated as:

$$(1 + C_m)\frac{\partial}{\partial t}\frac{\rho \langle \overline{u}_i \rangle}{n} + \frac{1}{n}\frac{\partial}{\partial x_j}\frac{\rho \langle \overline{u}_i \rangle \langle \overline{u}_j \rangle}{n} = -\frac{\partial \langle \overline{p} \rangle^f}{\partial x_i} - g_j x_j \frac{\partial \rho}{\partial x_i} + \frac{1}{n}\frac{\partial}{\partial x_j}\mu\left(\frac{\partial \langle \overline{u}_i \rangle}{\partial x_j} + \frac{\partial \langle \overline{u}_j \rangle}{\partial x_i}\right) + F_i \tag{4}$$

where C_m is the added mass coefficient to take the transient interaction between grains and water into account, n is the porosity, and $\langle \overline{p} \rangle^f$ is the volume averaged ensemble averaged pore pressure. Furthermore,

an additional term on the right hand side, F_i, was included to take account of the resistance force due to the presence of the porous media. The details of the derivation of the resistance force term were presented in Jensen et al. (2014) and is discussed further in the following section. Note the negative sign on the gravitational term on the right hand side which differs from that presented in Jensen et al. (2014) where it was mistyped as being positive.

Porous media resistance forces

When the momentum equation was volume averaged in the porous media, two terms arose representing frictional forces from the porous media and pressure forces (form drag) from the individual grains as shown in Jensen et al. (2014). Also Hsu (2002) and del Jesus et al. (2012) presented these terms. A closure model must be applied to describe the contributions from these terms as they cannot be resolved due to the volume averaging of the porous media. Here the extended Darcy-Forchheimer equation was applied, that includes linear and nonlinear forces as well as inertia forces to account for accelerations. The linear and nonlinear resistance forces were expressed as:

$$F_i = -a\rho\langle\overline{u}_i\rangle - b\rho\sqrt{\langle\overline{u}_j\rangle\langle\overline{u}_j\rangle}\langle\overline{u}_i\rangle \tag{5}$$

where a and b are resistance coefficients. These coefficients must be determined. Engelund (1954) formulated a relation between the resistance coefficients and the porosity, viscosity, and grain diameter for steady state flow, as also later included in Burcharth and Andersen (1995). These relations were included in the model presented by del Jesus et al. (2012). A similar expression to Engelund (1954) was formulated in van Gent (1995), where the effect of oscillatory flows was added to the expressions in terms of the KC-number. The latter formulations were applied in the model presented by Liu et al. (1999) and were also adopted and implemented in the present model. The resistance coefficients were formulated as:

$$a = \alpha\frac{(1-n)^2}{n^3}\frac{\mu}{\rho d_{50}^2} \tag{6}$$

$$b = \beta\left(1+\frac{7.5}{KC}\right)\frac{1-n}{n^3}\frac{1}{d_{50}} \tag{7}$$

where d_{50} is the grain diameter and $KC = u_m T/(nd_{50})$, where u_m is the maximum oscillating velocity and T is the period of the oscillation which in the following was set to the spectral peak period, T_p. α and β are empirical coefficients. Several values have been proposed for α and β in the literature e.g.van Gent (1995) who used $\alpha = 1000$ and $\beta = 1.1$, and Liu et al. (1999) who applied $\alpha = 200$ and $\beta = 1.1$. In Jensen et al. (2014) a calibration was performed including a greater range of flow regimes than previously seen and values of $\alpha = 500$ and $\beta = 2.0$ were proposed. These are applied in the following.

Finally, the inertia term in the extended Darcy-Forchheimer equation was included in Eq. (4) through C_m, which van Gent (1995) gave as:

$$C_m = \gamma_p\frac{1-n}{n} \tag{8}$$

where γ_p is an empirical coefficient, which takes the value 0.34.

Free surface VOF modelling

The interface tracking of the free water surface was conducted using a volume of fluid approach (VOF), where the specific details are given in Berberović et al. (2009). The tracking was resolved by the solution to:

$$\frac{\partial\alpha}{\partial t} + \frac{1}{n}\frac{\partial}{\partial x_i}\left(\langle\overline{u}_i\rangle\alpha\right) + \frac{1}{n}\frac{\partial}{\partial x_i}\left(\langle\overline{u}_i^r\rangle\alpha(1-\alpha)\right) = 0 \tag{9}$$

where α is 1 for water and 0 for air. $\langle\overline{u}^r\rangle = \langle\overline{u}^f\rangle - \langle\overline{u}^a\rangle$ is a relative velocity between the fluid and the air as described in Berberović et al. (2009). The last term is denoted the compression term and handles the compression of the interface between fluid and air. This term vanishes in the fluid ($\alpha = 1$) and in the air ($\alpha = 0$), and is only active in the interface region of the free surface. Note that the $1/n$ terms have to be included to account for the fact that a given volume is filled/emptied faster, when a sediment grain takes up part of the volume.

IRREGULAR SEA STATE CREST HEIGHT DISTRIBUTION

The irregular sea state was generated by super-position of a number of regular linear wave components. As such it is of interest to evaluate whether the irregular waves observed in the numerical wave flume resembles the actual crest height distribution to be expected in a real natural sea state. This is also a question of relevance for physical model testing where irregular sea states are often generated based on linear wave theory, see e.g. Schäffer et al. (1994). The crest height distribution for an irregular sea state can be expressed by different empirical relations. The most common are the Weibull and Rayleigh distributions. In Forristall (2000) it was shown that for wave conditions with more non-linear wave components these distributions may not give the best description. Here the Forristall distribution was proposed which takes into account a higher degree of non-linearity.

In order to verify the statistical distribution of crest heights an irregular sea state was generated in an empty numerical wave flume on a flat horizontal bed. The domain had a length of 1000 m and a heights of 70 m with the water depth maintained at $h = 35$ m. The waves were generated based on a JONSWAP spectrum with a significant wave height, $H_s = 9.0$ m and a peak wave period, $T_p = 11.0$ s. Wave generation was based on Jacobsen et al. (2012) where relaxation zones were applied with an inlet relaxation zone of 200 m and an outlet relaxation zone of 150 m.

Figure 1 presents the distribution of crest height, C, compared to the Rayleigh and Forristall distribution. Five different positions in the wave flume are presented. The crest heights were found to be overestimated compared to the Rayleigh distribution whereas the Forristall distribution was found to provide a better estimate of the simulated crest heights. As such the statistical distribution of the waves was comparable to a realistic irregular sea state.

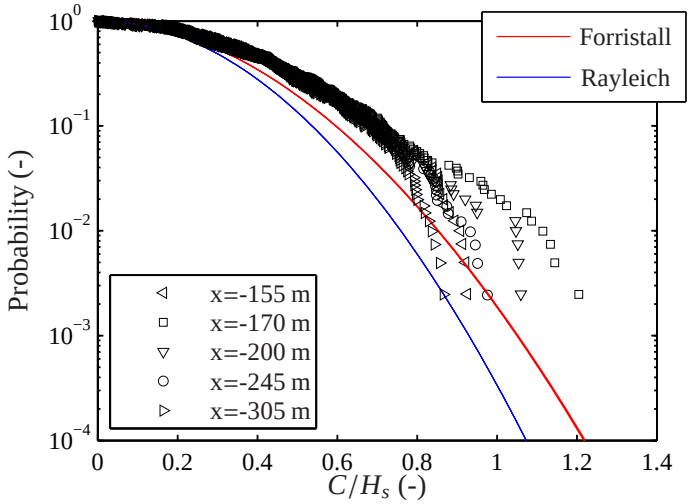

Figure 1: Crest height, C, distribution for a significant wave height at $H_s = 9.0$ m and a peak period at $T_p = 11.0$ s. The x-values corresponds to the wave gauge position in the flume where $x = 0$ is positioned 600 m from the inlet boundary.

It is noted that the irregular time series for the present simulations were composed by a number of wave component equally distributed across the frequency domain. This means that the same number of wave components were included for e.g. the high frequency part of the wave spectrum as for the area around the peak frequency. Another approach is to cluster the wave components at the frequencies which contains the most energy in the wave spectrum, i.e. around the peak frequency. This may affect the overall wave distribution and the wave-wave interaction in the irregular sea state and thereby provide a more realistic representation of the wave distribution. This was not investigated in the present study.

TWO-DIMENSIONAL SCREENING

The first step in the proposed methodology was to perform the two-dimensional screening where the parameters of interest were evaluated for the complete irregular time series. The example applied in the present paper was a breakwater in deep water exposed to irregular sea states. Figure 2 presents a cross

section of the breakwater with the different structural parts. The focus in the present study was the forces on the concrete sea-wall which may cause sliding or over-turning if they are not taken correctly into account during the design phase.

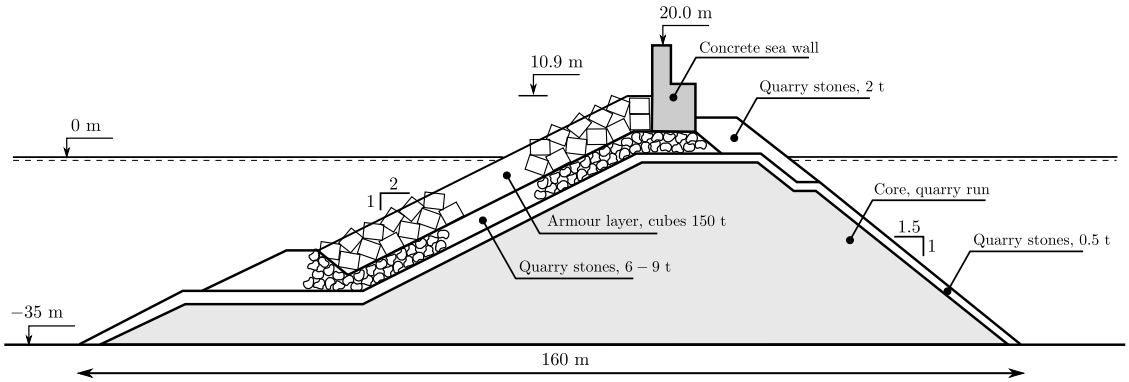

Figure 2: Sketch of the Bilbao breakwater profile. After Jensen (1984).

The model was setup with a distance from the inlet boundary to the toe of the breakwater at 600 m. The distance from the leeward side of the breakwater to the outlet was 240 m. The height of the domain was 70 m. Relaxation zones were added at the inlet and outlet for wave generation and absorption with a length at 200 m and 150 m respectively. A uniform grid size of 1.0 m was used in the domain. Grid refinement was applied around and inside the breakwater structure with a grid size at 0.25 m in all directions. A total of $100,000$ grid cells were applied. The total simulation lasted 3 hours which yields 720-1000 waves depending on the wave period. Each simulation was completed with parallel computation on eight processor cores in approximately 48 h. The porosity module was applied with resistance coefficients set to $\alpha = 500$ and $\beta = 2.0$ according to the calibration results given in Jensen et al. (2014) and the KC-number defined with the peak wave period, T_p.

The breakwater profile was investigated for a number of wave conditions described in Burcharth et al. (1995). All simulations were performed in prototype. Irregular waves were generated based on a JONSWAP wave spectrum with peak enhancement factor, $\gamma = 3.3$. The significant wave height was $H_s = [8, 9, 10, 11]$ m with a peak wave period of $T_p = 15$ s. The wave condition with $H_s = 8$ m was further tested for a peak wave period at $T_p = [10, 17, 21]$ s and $H_s = 11$ m for $T_p = [17, 19]$. These choices gave wave steepnesses in the interval 0.02 to 0.05 where the steepness was evaluated as $H_s/1.56T_p^2$ for deep-water conditions.

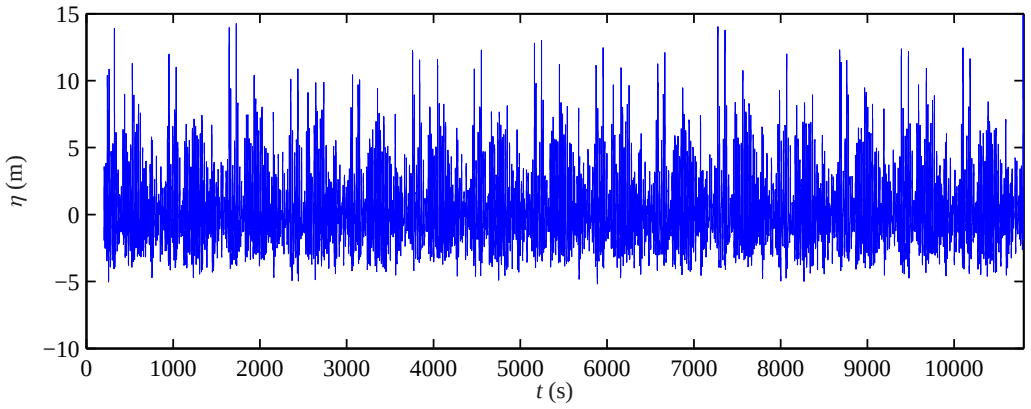

Figure 3: Surface elevation for the complete three hour irregular sea state for a significant wave height at $H_s = 9.0$ m and a peak period at $T_p = 15.0$ s.

Figure 4 presents the incident and reflected wave spectra for one wave condition. The incident wave spectrum was found from the surface elevation recorded at an offshore position at a distance of 200 m from

the toe of the breakwater. It should be noted that the spectrum has an extra peak at approximately 0.1 Hz which is not the case for the standard JONSWAP spectrum. This is due to the fact that the irregular wave generation was achieved by superposition of a number of linear regular wave components. As the waves propagate from the inlet boundary towards the breakwater higher harmonics are introduced, which lead to the second peak in the wave spectrum.

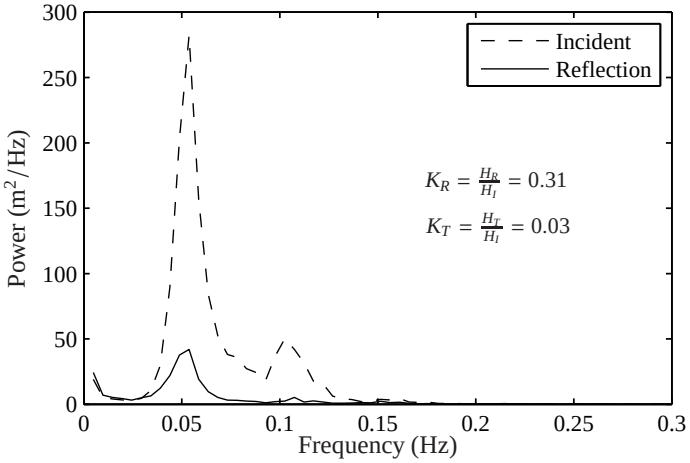

Figure 4: Wave spectra for incident and reflected waves for an incident significant wave height at H_s = 10.0 **m and a peak period at** T_p = 15.0 **s.**

The reflection coefficient was found as the ratio between reflected and incident significant wave height based on the method described in Zelt and Skjelbreia (1992) for separating incident and reflected wave fields. In this work five wave gauges were applied for separating the incident and reflected waves. The results for all simulated cases are shown in Figure 5 as a function of the breaker (surf-similarity) parameter, $\zeta_0 = \tan\alpha / \sqrt{S_0}$, where S_0 is the wave steepness based on the spectral period $T_{m-1.0} = m_{-1}/m_0$ and the significant wave height at the toe of the breakwater. The results were compared to the empirical relation given in Zanuttigh and Van der Meer (2006). The simulated reflection coefficients were found to compare well with the empirical relation and as such the selected case and the numerical model provides a realistic representation of the wave-structure interaction with a rubble mound breakwater.

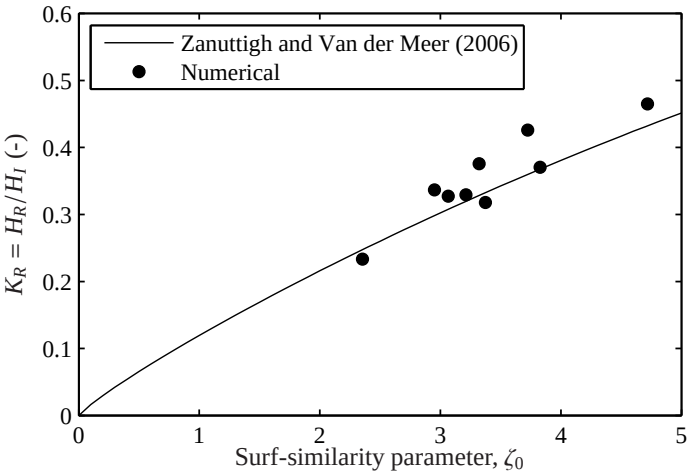

Figure 5: Reflection coefficients for the Bilbao test case. Comparison with empirical relation presented in Zanuttigh and Van der Meer (2006)

.

The forces on the sea-wall were computed throughout the 3 hours simulation by integrating the pressure on the surface of the wall. In the following the forces and the subsequent reproduction of the extreme events are shown for the sea state with H_s = 11 m and T_p = 19 s. Figure 6 presents the time series for a typical impact load in terms of the horizontal and vertical forces. The time variation of the horizontal force resembled the so-called "church roof" force variation, which is characteristic for wave impacts on a vertical wall. This was shown in for example Bullock et al. (2007) and Bredmose et al. (2009). The first part of the impact originates from the impact of the main body of water causing an impulsive load with a very short duration and a large magnitude. This is followed by the hydrostatic load from the water column in front of the sea-wall as the water initiates the run-down stage.

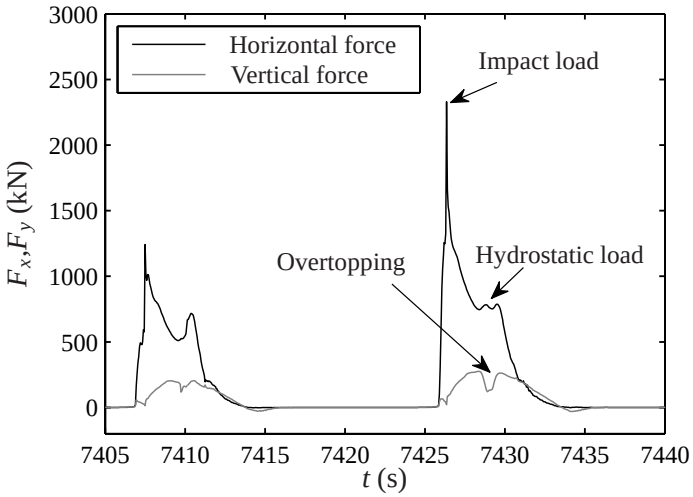

Figure 6: Impact event on the breakwater sea-wall.

.

Figure 7 presents the pressure contours during the impact event where the approach, run-up, impact and run-down stages are illustrated. At run-down it is seen how the next incoming wave interacts with the run-down and thereby causing wave breaking along the breakwater slope. This shows how the run-up stage, and thereby the impact on the sea-wall, depends on the approaching wave but also the run-down of the previous wave.

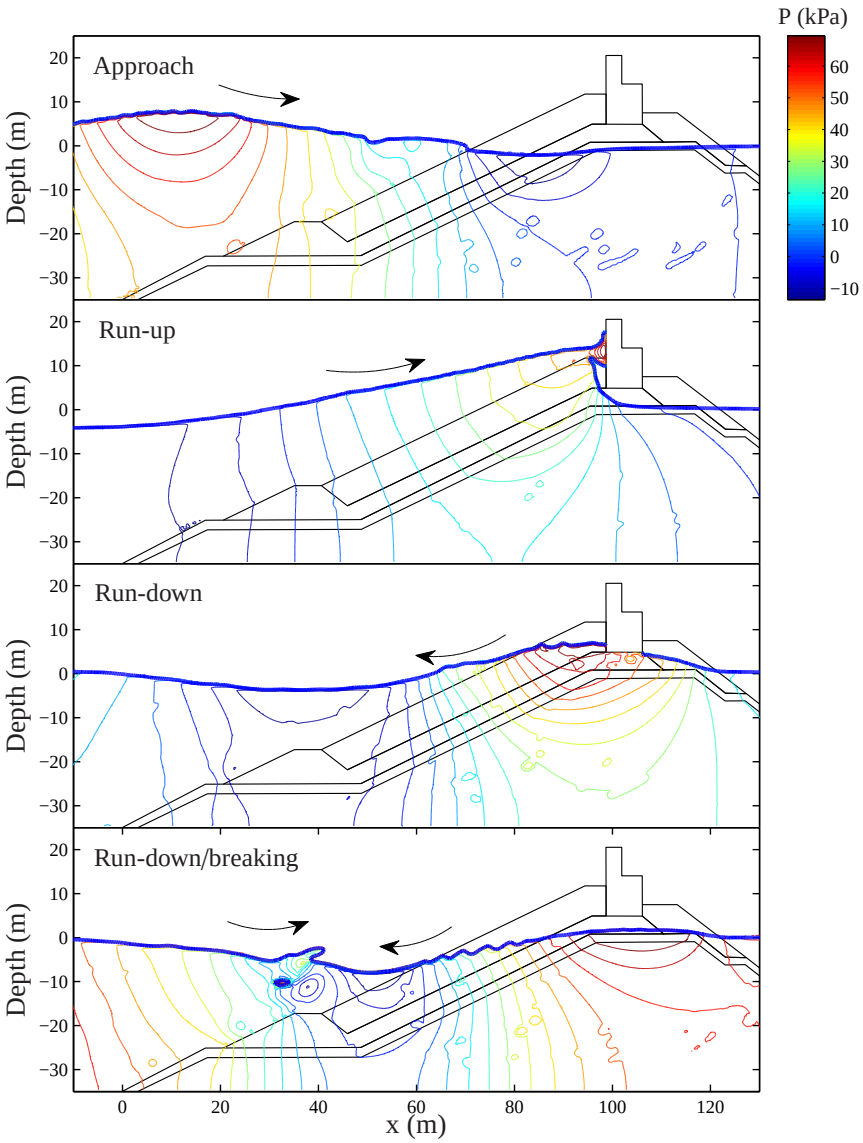

Figure 7: Pressure contours for an impact event on the sea-wall represented by the approach, run-up and run-down stages.

TWO-DIMENSIONAL REPRODUCTION OF EXTREME EVENTS

The procedure for reproducing extreme events was validated by selecting three events of impact on the sea-wall. These were reproduced in a short sequence in the two-dimensional model. The irregular wave generation was started with a phase offset, ϕ, defined as:

$$\phi = cx + NT_p \tag{10}$$

where c is the wave celerity taken as $c = \sqrt{gh}$, x is the distance from the inlet boundary to the point of reproduction, T_p is the peak wave period, and N is the number of peak wave periods to apply as warm-up. Values of $N = 1 - 5$ was applied for validating the method. The reproduced event was compared to the corresponding event form the complete irregular time series in terms of the water surface elevation at the toe of the breakwater and the horizontal forces on the sea-wall super-structure.

Figure 8 presents the surface elevation at the offshore location in front of the breakwater. The target surface elevation represents the entire irregular time series. The short reproductions are denoted by the factor N as given in Eq. (10). For a short warm-up period of $N = 1$ the surface elevation was in general not reproduced correctly. The surface elevation before the extreme event was in general not captured. Also at the peak of the surface elevation some discrepancies were seen. At $N = 4$ and $N = 5$ a good agreement was found between the target time series and the reproduced sequence. Also the variation of the free surface before and after the extreme target wave was reproduced with $N = 4$ and $N = 5$. This is of relevance for reproducing the forces on the breakwater sea-wall due to a run-up event. The run-up is a result of the interaction of the different wave components as they approach the breakwater and as such, not only the one extreme event needs to be reproduced correctly.

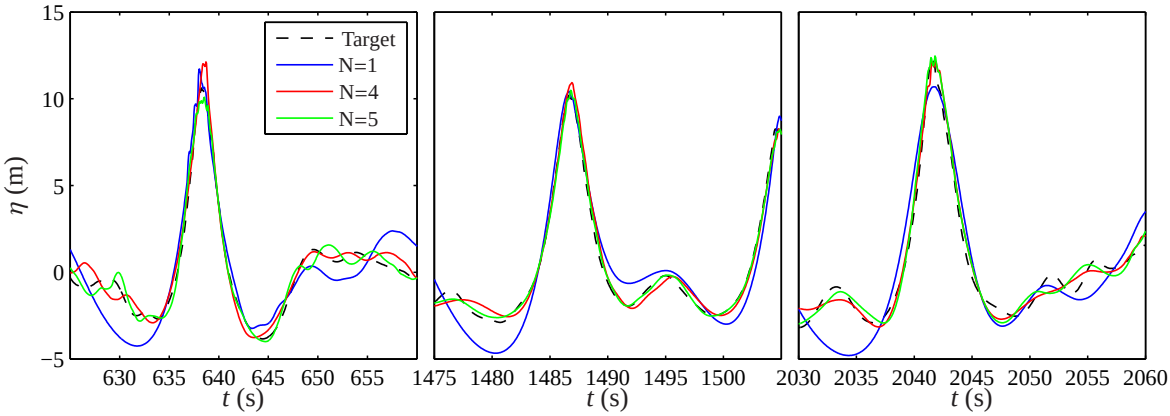

Figure 8: Surface elevation in front of the breakwater for three impact events. The target represents the surface elevation from the full irregular time series which is compared to the short reproductions.

.

In Figure 9 the horizontal forces on the sea-wall for the three impact events are presented. As for the surface elevation the short warm-up period of $N = 1$ gives a less accurate reproduction of the forces. For $N = 4$ and $N = 5$ better agreement was seen although the level of agreement was still slightly lower than for the comparisons of the free water surface elevation.

It is noted, that the reproduction of en short event does not correctly reproduce the internal setup of the phreatic level. In Wellens and van Gent (2012) a numerical model was applied to show how the internal setup develops during an irregular sea-state and is governed by e.g. the wave height to stone diameter ratio, H_s/D_{n50}. For the present cases of extreme run-up events the internal setup was assumed to have a minor effect on the maximum run-up due to the relatively large stone material sizes which reduces the setup.

For the present example the flow conditions in front of the breakwater is very much affected by the relatively high reflection of energy from the breakwater itself. As such the surface elevation and forces on the sea-wall is also depending on the conditions previous to the actual extreme event. It is expected that for cases with less reflection, e.g. wave impacts on mono-piles or jacket structures, the warm-up period may be reduced compared to the present case.

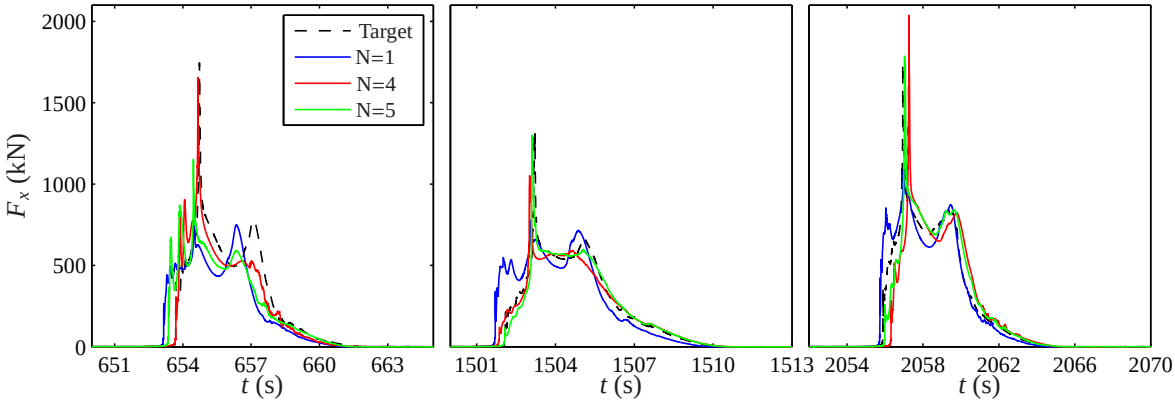

Figure 9: Horizontal forces on the sea-wall of the breakwater for three impact events. The target represents the forces from the full irregular time series which is compared to the short reproductions.

.

THREE-DIMENSIONAL REPRODUCTION - OBLIQUE WAVE INTERACTION

The impact events that were reproduced in the previous section as short sequences were applied to investigate the effect of oblique waves on the sea-wall impact forces. For this a three-dimensional model setup is required. The model domain applied for the two-dimensional screening was extended in the transversal direction and the breakwater was rotated by an angle of 30°. The layout of the three-dimensional model domain is shown in Figure 10.

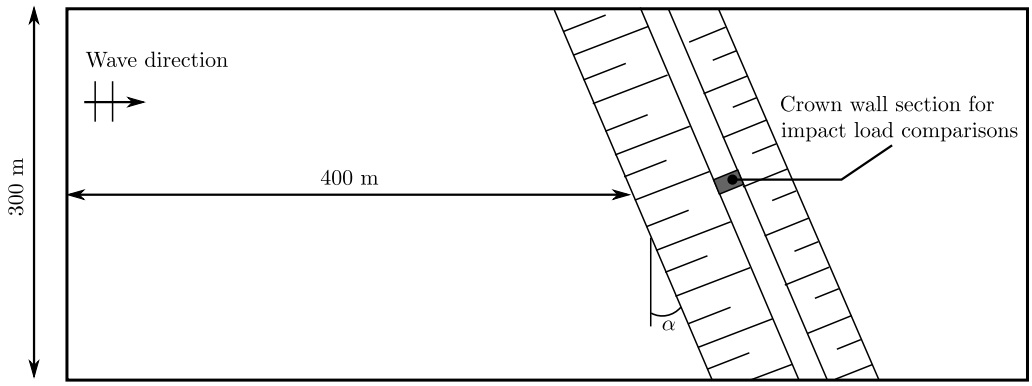

Figure 10: Layout of the three-dimensional model domain for oblique wave interaction.

The model domain covered the same distance upstream and downstream the breakwater structure as for the 2D screening model. In the transversal direction a distance of 300 m was included. The same grid resolution was maintained as for the 2D models. A total of $\approx 10^6$ grid cells was applied. Each simulation was completed with parallel computation on 40 processor cores in approximately 96 h.

Figure 11 presents the time series of the horizontal forces for the three impact events as shown in Figure 9. The results are shown for the case with an incident wave angle of attack of 0°, i.e. head-on, and for an oblique wave with an angle of attack of 30°. The effect of the oblique wave was clear in terms of a reduced impact peak load. The wave travelled along the breakwater and the sea-wall which removed the direct impact that caused the peak load for head-on waves. For the simulated extreme events the peak load was in general reduced by 25 – 50 %. Figure 12 shows the free surface in-front of the breakwater. The run-up event that impacts the sea-wall moves along the breakwater and only interacts with the sea-wall at a relatively short section at a given time.

The effect of oblique waves was evaluated based on the forces on one section of the sea-wall as shown in Figure 10. It is expected that the forces varies along the length of the breakwater i.e. there is a spatial

variation. This was shown in Lara et al. (2012b) for the forces on a vertical impermeable breakwater exposed to oblique waves. In the present work the spatial variation was not addressed although it is expected that the reduction of the horizontal impact forces as found in the present simulations may also show some variation along the length of the breakwater.

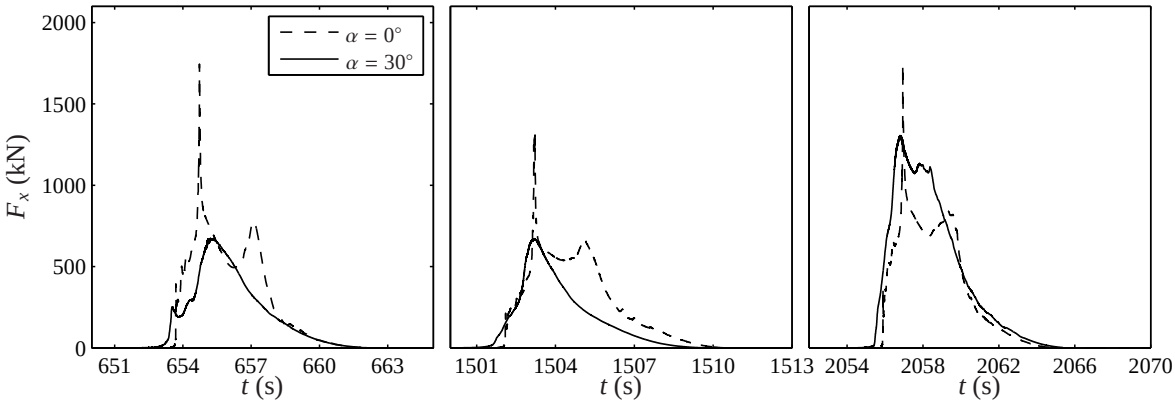

Figure 11: Effect of oblique waves on horizontal forces on the sea-wall of the breakwater.

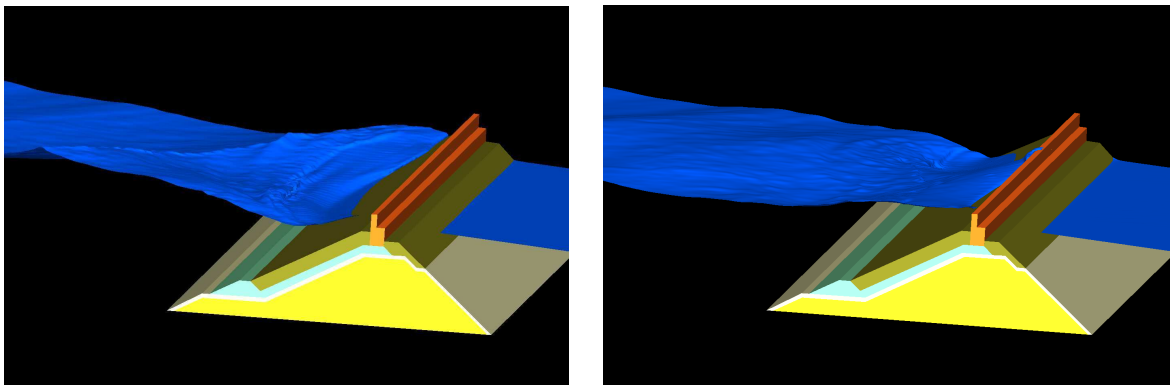

Figure 12: Visualization of the free surface during wave impact on the sea-wall.

CONCLUSIONS

This paper presented the combination of a two-dimensional screening process for irregular wave conditions and a three-dimensional reproduction of an extreme event originating from the irregular sea state. This combination greatly enhances the efficiency of the CFD model in terms of a reduction in the computational time as compared to simulating a complete irregular sea state in a three-dimensional setup.

The main conclusions are summarised as:

1. The numerical model was found to provide a reasonable reproduction of the crest height distribution in an irregular sea state. The best fit was found by comparing to the empirical Forristall distribution although some improvements can be made.

2. Good agreement was found between the surface elevation from the entire irregular sea state and the short reproduction sequences applying a warm-up period of $4T_p$

3. The horizontal forces on the sea-wall were also reproduced with good agreement although slightly more variation was seen compared to the reproduction of the surface elevation.

4. For the simulations of the extreme events with oblique waves with an incident angle of 30° the peak impact load was reduced by 25 – 50 %.

The work presented in the present paper aimed at providing a general validation of the methodology for reproducing extreme events from an irregular sea state in a short sequence based on a phase offset of the wave generation signal. Although the methodology is based on a numerical investigation the method is also of relevance, and applicable, in relation to physical model experiments. In cases where a specific impact event needs to be repeated e.g. for testing different structural configurations or for providing better statistical data basis for the extreme value analysis it may be more time efficient to apply the presented methodology.

The method was applied for investigating the effect of oblique waves on the sea-wall forces on a rubble mound breakwater. Only a limited number of simulations were performed which did not cover the entire parameter space which may be of interest. It is recommended to further expand the investigations initiated in this paper to cover a range of incident wave angles, wave conditions etc. This will give a more complete understanding of the effect of oblique waves on the forces on breakwater super-structures exposed to extreme run-up and impact events.

ACKNOWLEDGEMENTS

The support of the Danish Ministry of Science, Technology and Innovation through the GTS grant: Fremtidens Marine Konstruktioner (Marine Structures of the Future), is acknowledged.

REFERENCES

Antohe, B. V. and Laget, J. L. (1997). A general two-equation macroscopic turbulence model for incompressible flow in porous media. *International Journal of Heat and Mass Transfer*, 40(13):3013–3024.

Berberović, E., van Hinsberg, N., Jakirlić, S., Roisman, I., and Tropea, C. (2009). Drop impact onto a liquid layer of finite thickness: Dynamics of the cavity evolution. *Physical Review E*, 79(3).

Bredmose, H., Peregrine, D. H., and Bullock, G. N. (2009). Violent breaking wave impacts. Part 2: modelling the effect of air. *Journal of Fluid Mechanics*, 641:389.

Bullock, G., Obhrai, C., Peregrine, D., and Bredmose, H. (2007). Violent breaking wave impacts. Part 1: Results from large-scale regular wave tests on vertical and sloping walls. *Coastal Engineering*, 54(8):602–617.

Burcharth, H. and Andersen, O.H. (1995). On the one-dimensional steady and unsteady porous flow equations. *Coastal Engineering*, 24(3-4):233–257.

Burcharth, H., Frigaard, P., Uzcanga, J., Berenguer, J., Madrigal, B., and Villanueva, J. (1995). *Design of the Ciervana Breakwater*.

del Jesus, M., Lara, J. L., and Losada, I. J. (2012). Three-dimensional interaction of waves and porous coastal structures Part I: Numerical model formulation. *Coastal Engineering*, 64:57–72.

Engelund, F. (1954). On the laminar and turbulent flows of ground water through homogeneous sand. Technical report, Danish Academy of Technical Sciences.

Forristall, G. Z. (2000). Wave Crest Distributions: Observations and Second-Order Theory. *Journal of physical oceanography*, pages 1931–1943.

Higuera, P., Lara, J. L., and Losada, I. J. (2014a). Three-dimensional interaction of waves and porous coastal structures using OpenFOAM®. Part I: Formulation and validation. *Coastal Engineering*, 83:243–258.

Higuera, P., Lara, J. L., and Losada, I. J. (2014b). Three-dimensional interaction of waves and porous coastal structures using OpenFOAM®. Part II: Application. *Coastal Engineering*, 83:259–270.

Hsu, T. (2002). A numerical model for wave motions and turbulence flows in front of a composite breakwater. *Coastal Engineering*, 46(1):25–50.

Jacobsen, N. G., Fuhrman, D. R., and Fredsøe, J. (2012). A wave generation toolbox for the open-source CFD library : OpenFoam®. *International Journal for Numerical Methods in Fluids*, 70:1073–1088.

Jacobsen, N. G. and Fredsøe, J. (2014). Cross-Shore Redistribution of Nourished Sand near a Breaker Bar. *Journal of Waterway, Port, Coastal, and Ocean Engineering*, (March/April):125–134.

Jensen, B., Jacobsen, N. G., and Christensen, E. D. (2014). Investigations on the porous media equations and resistance coefficients for coastal structures. *Coastal Engineering*, 84:56–72.

Jensen, O. J. (1984). *A Monograph on Rubble Mound Breakwaters*. Danish Hydraulic Institute, Agern Alle 5, DK-2970 Hoersholm, Denmark.

Lara, J. L., del Jesus, M., and Losada, I. J. (2012a). Three-dimensional interaction of waves and porous coastal structures Part II: Experimental validation. *Coastal Engineering*, 64:26–46.

Lara, J. L., Higuera, P., Maza, M., del Jesus, M., Losada, I. n. J., and Barajas, G. (2012b). Forces induced on a vertical breakwater by incident oblique waves. In *International Conference on Coastal Engineering*, pages 1–10.

Liu, P. L.-F., Lin, P., Chang, K.-A., and Sakakiyama, T. (1999). Numerical modeling of wave interaction with porous structures. *Journal of Waterways, Port, Coastal and Ocean Engineering*, 125:322–330.

Matsumoto, A., Mano, A., Mitsui, J., and Hanzawa, M. (2012). Stability prediction on armor blocks for submerged breakwater by computational fluid dynamics. In *International Conference on Coastal Engineering*, pages 1–14.

Nakayama, A. and Kuwahara, F. (1999). A macroscopic turbulence model for flow in a porous medium. *Journal of fluids engineering*, 121(June):427–433.

Schäffer, H., Stolborg, T., and Hyllested, P. (1994). Simultaneous generation and active wave absorption of waves in flumes. In *Proc. Int. Symposium: Waves-Physical and Numerical Modelling*, pages 90–99. Univ. British Colombia, Vancouver, Canada.

Stahlmann, A. and Schlurmann, T. (2012). Investigations on scour development at tripod foundations for offshore wind turbines: modeling and application. In *International Conference on Coastal Engineering*, pages 1–11.

van Gent, M. R. A. (1995). Porous Flow through Rubble-Mound Material. *Journal of Waterway, Port, Coastal, and Ocean Engineering*, 121(3):176–181.

Wellens, P. and van Gent, M. (2012). Wave-induced setup inside permeable structures. In *International Conference on Coastal Engineering*, pages 1–14.

Zanuttigh, B. and Van der Meer, J. (2006). Wave reflections from coastal structures. In *International Conference on Coastal Engineering*, pages 1–13.

Zelt, J. A. and Skjelbreia, J. E. (1992). Estimating incident and reflected wave fields using an arbitrary number of wave gauges. In *International Conference on Coastal Engineering*, pages 777–789.